ORIGINAL RESEARCH PAPER

Design and analysis of photonic crystal ring resonator based 6 × 6 wavelength router for photonic integrated circuits

Sridarshini Thirumaran[1] | Shanmuga Sundar Dhanabalan[2] | Indira Gandhi Sannasi[1]

[1]Department of Electronics, Madras Institute of Technology, Chennai, Tamil Nadu, India

[2]Laboratorio de superficies y Nanomateriales, Facultad de Ciencias Físicas y Matemáticas, Universidad de Chile, Santiago, Chile

Correspondence

Sridarshini Thirumaran, Department of Electronics, Madras Institute of Technology, Chennai, Tamil Nadu, India.
Email: sridarshiniv@gmail.com

Abstract

A photonic crystal ring resonator-based 6 × 6 router has been designed and reported. The router is designed using silicon pillars with a refractive index of 3.47 perforated in the air background of refractive index 1 in a square lattice with a lattice constant of $a = 562$ nm. The router is designed to operate in the third optical window wavelength which has low loss and most widely used in optical communication systems and networks. Plane-wave expansion and finite difference time domain method has been used to obtain the bandgap and performance of the designed router, which exhibits acceptable performance such as low insertion loss, low propagation delay, and low crosstalk. These routers will find applications in the photonic integrated circuit that paves a path to all-optical networks.

1 | INTRODUCTION

Photonic integrated circuit (PIC) is the future technology in which all the optical components and devices are integrated to form a single photonic chip. These chips will satisfy the demands for signal processing and high-speed data transmission between the increasing numbers of users. These miniaturised PIC with high reliability, minimised errors, and high speed of operation will highly enhance the light wave communications [1]. This eventually entails routing of signals between different ports in the integrated circuit networks with complete connectivity and improved performance [2]. Photonic crystal-based components such as splitters [3,4], circulators [5], filters [6], decoder [7], low-power encoders [8–10], and routers [11–13] were designed and reported. Among them, routers play a vital role in transmitting signals from one user to others with low loss and high efficiency in order to deliver high-quality signals to the end-users and minimise the traffic in the data transmission.

The 3 × 3 router with two different topologies interconnecting three input and output ports was reported. Trade-off between the complexity of the structure and wavelength resource has been considered in designing the routers [2]. The 4 × 4 dynamic hitless router on Silicon on Insulator (SOI) technology using eight micro-ring resonators which were individually tuned using micro-heaters was demonstrated. The design has an extinction ratio of 20.79 dB and a bandwidth of 38.5 GHz [11]. The 4 × 4 crossbar based on micro-ring resonator add-drop filter using waveguides and ring resonators of radii as small as 1.8 μm fabricated on SOI substrate using deep UV lithography [14]. Kirman and Martínez proposed an all optical approach to construct data networks on chip that combines wavelength-based routing with high on-chip bandwidth, less power, and robust [15].

A five-port optical router based on micro-ring resonators on SOI platform using standard CMOS technology was reported. These resonators can be tuned through the thermo-optic effect and extinction ratio of 21 dB was reported [16]. Calo and Petruzzelli proposed an optical 1 × 2 passive wavelength router and also analysed the behaviour of a 4 × 4 router configuration by assembling eight 1 × 2 routers which are capable of connecting four transmitters and four receivers with maximum crosstalk of −13.9 dB between the ports [17]. Moreover, in 2014 they have proposed a 2 × 2 PhC router using two photonic crystal ring resonator (PCRR) of 3.2 μm diameter and a broadband PhC waveguide with the maximum crosstalk of −20 dB. Analysis of 4 × 4 router using a four 2 × 2 router is also been reported [18].

Broadband PhC waveguide crossing using two 1 × 2 PhC λ-routers based on point defect micro cavities was demonstrated. High routing efficiency was achieved by engineering the rods of micro-cavity structure with gradual radii [12]. An optical switched router using 16 microrings, 14 crossrings, and 4 90° waveguide bends to construct a large
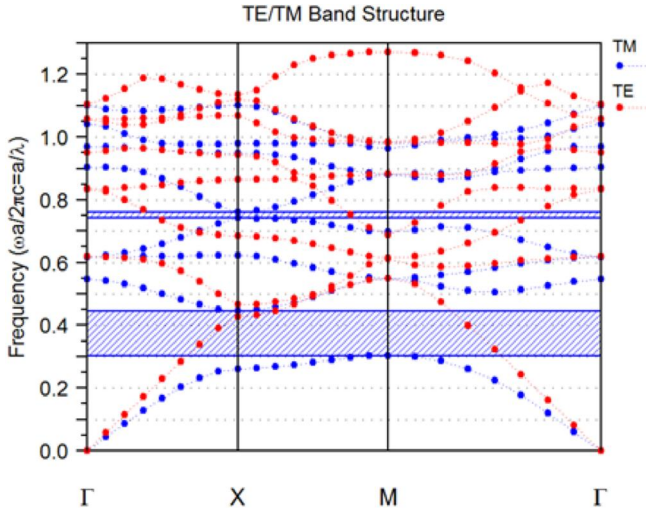
FIGURE 1 Photonic band gap for Si rods with RI 3.47 in air background

photonic routing network on chips was reported [13]. Sathyadevaki et al, have demonstrated 4 × 4 wavelength routers which exhibit maximum crosstalk of −15.1017 dB at 1567 nm and maximum insertion loss of 1.73 dB at 1520 nm [19]. The photonic crystal-based routers using different optical materials like Germanium, Gallium arsenide, and Indium phosphate was reported and the performance of the router with respect to the materials were also analysed and reported [20].

Even though considerable research has been carried out in design, size and performance of routers on different configurations from 1 × 2 router to 4 × 4 router with low crosstalk, low insertion loss, and high efficiency, the 6 × 6 routers with maximum insertion loss of 1.6115 dB and crosstalk of −12.3553 dB with highest propagation delay of 810 ps is reported for the first time. The 6 × 6 router was designed using the 1 × 2 and 2 × 2 routers as a basic building block and the entire structure is analysed using the finite difference time domain (FDTD) method.

2 | PHOTONIC BANDGAP STRUCTURE

The router is designed with silicon rods embedded in air background with an index difference of 2.46 in a square lattice arrangement with a lattice constant of $a = 562$ nm. The square lattice is preferred to obtain the symmetrical structural design and well confined photonic bandgap (PBG) in this design [21]. The gap map technique was used to obtain the optimised design parameters such as lattice constant 'a', rod radius 'r'. Gap map is a plot of the PBG of crystals by varying one or more parameters of the crystals [22]. The radius of the Si rods ($r = 0.175{*}a$ μm) and the lattice constant 'a' were obtained from the gap map technique for the wavelength of 1550 nm. Figure 1 shows the PBG structure of the proposed router design.
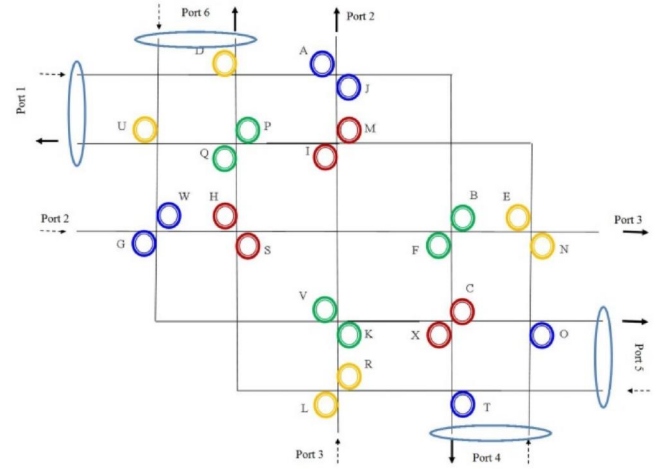
FIGURE 2 Schematic of 6 × 6 wavelength router topology

TABLE 1 Routing elements and their respective wavelength used for the routing between the ports

	Output ports					
	1	2	3	4	5	6
Input ports						
1		A-λ_1	B-λ_2	No R-λ_3	C-λ_4	D-λ_5
2	E-λ_5		No R-λ_3	F-λ_2	G-λ_1	H-λ_4
3	I-λ_4	No R-λ_3		J-λ_1	K-λ_2	L-λ_5
4	No R-λ_3	M-λ_4	N-λ_5		O-λ_1	P-λ_2
5	Q-λ_2	R-λ_5	S-λ_4	T-λ_1		No R-λ_3
6	U-λ_5	V-λ_2	W-λ_1	X-λ_4	No R-λ_3	

Abbreviation: No R, no ring resonator.

3 | ROUTER DESIGN AND TOPOLOGY

The 6 × 6 PCRR-based router comprises of 24 ring resonators with a dense arrangement. The router is designed to operate in the third window due to its low attenuation loss and widely used optical window. Figure 2 shows the pictorial representation of 6 × 6 routers. The routing of the wavelength between the 6 inputs and output ports were achieved by using the four 1 × 2 and ten 2 × 2 routers. Table 1 shows the routing element and their respective wavelength used for the link establishment for all 30 pathways in 6 × 6 wavelength router. The proposed router requires 24 ring resonators (named from A to X) to route the four out of five wavelengths whereas the remaining one doesn't need resonators to route between the ports. Each ring resonator is designed to have specific resonant wavelengths to enhance the transmission. Four groups of six resonators have been clubbed to have one resonant wavelength for operation.

Table 2 shows the resonating wavelength and rod radius of the ring resonators used in this design. The resonant wavelength of the designed ring resonators depends on the rod radius of the resonator. The value of 'r' is optimised using the

Resonators	Radius of the rods (μm)	Resonating wavelength (μm)
A, G, J, O, T, W	0.070	$\lambda_1 = 1.49$
B, F, K, P, Q, V	0.071	$\lambda_2 = 1.50$
None	—	$\lambda_3 = 1.48$
C, H, I, M, S, X	0.073	$\lambda_4 = 1.51$
D, E, L, N, R, U	0.075	$\lambda_5 = 1.52$

TABLE 2 Resonating wavelength and rod radius of the ring resonators of 6×6 wavelength router

gap map technique to get a desired resonant wavelength. A gap map representing TE/TM gap locations versus the ratio of rod radius to the lattice constants, as shown in Figure 3a is used for the optimization process. From the obtained gap map plot the value of the inner rod radius is chosen accordingly to resonate the required wavelength. A curve showing the calculated resonant wavelength as a function of the rod radius is plotted as shown in Figure 3b.

The wavelengths from the third window 1.49, 1.5, 1.51, and 1.52 μm were used for the routing. Resonators A, G, J, O, T, and W resonate for $\lambda_1 = 1.49$ μm. B, F, K, P, Q, and V resonators form the second group resonating at $\lambda_2 = 1.5$ μm. The third group of resonators C, H, I, M, S, and X resonates at $\lambda_4 = 1.51$ μm and finally D, E, L, N, R, and U is designed to have a resonant wavelength of $\lambda_5 = 1.52$ μm. λ_3 is been selected as 1.48 μm from the PBG range and it does not require any resonating structures to route them.

In order to have a better understanding, the routing of wavelength by considering port 2 as the input port is explained in detail with respective figures. With λ_1 as wavelength, the signal from port 2 will resonate at ring resonator G and will appear as an output signal at port 5. The wavelength λ_2 from port 2 will travel in the straight waveguide and then resonates with ring resonator F to reach output port 4.

The wavelengths λ_4 and λ_5 will resonate at the ring resonator H and E and reaches the output ports 6 and 1 respectively. Port 2 to output port 3 does not requires any resonators and λ_3 signals will propagate in the straight waveguide without encountering any ring resonator to reach the port 3. Similar to this the other wavelengths will propagate from different input ports using their respective routing path to reach the desired destination ports. The routing path depends on the input wavelength and the resonant wavelength of the resonators placed in the path. The propagation path (routing path) for the input/output ports in the structure is based on the location of the ring resonators for each wavelength. Figures 4–8 show the propagation of signal with port 2 as input to different output ports.

4 | SIMULATION RESULTS

Performance of 6×6 wavelength router is analysed using the FDTD method with perfectly matched layer boundary conditions. Courant condition is used to obtain stable results at each simulation with a Gaussian wave as an input signal [23]. The parameters such as propagation delay, insertion loss, and
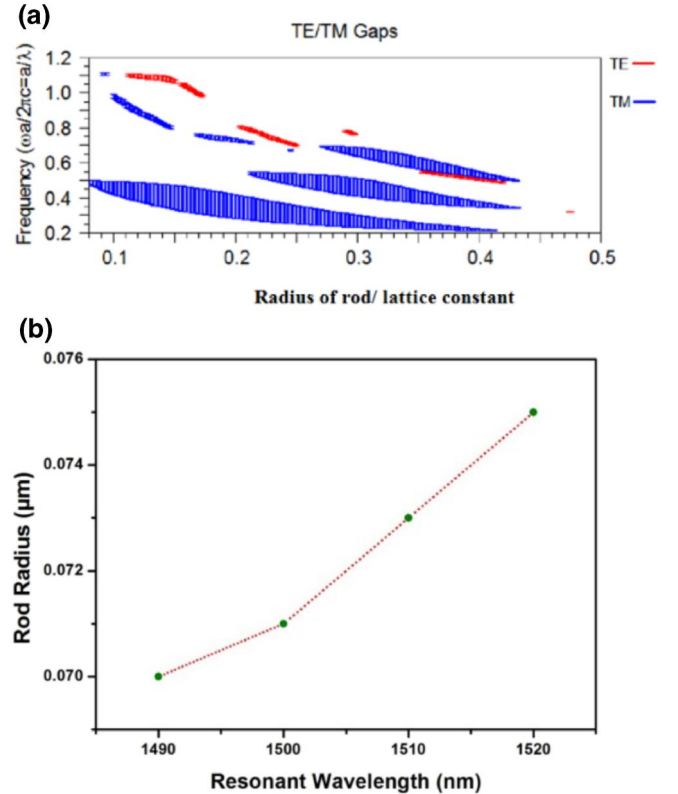
FIGURE 3 (a) Gap map plot for Si rods in air background with square lattice arrangement. (b) Variation of resonant wavelength with respect to the rod radius

crosstalk were calculated using the standard formulae [2]. Propagation delay is obtained by using numerical analysis from FDTD simulations. Crosstalk is the phenomenon in which a signal transmitted on one channel of a transmission system creates an undesired effect in another channel. Insertion loss is the amount of light that is lost as the signal arrives at the receiving end of the link. Insertion loss is measured in decibels (dB) and each passive connection in a system increases the dB loss for the system as a whole. Transmittance at all the output ports was obtained then the crosstalk and insertion losses were calculated using the following expressions.

$$\text{Crosstalk (dB)} = (T_i - T_t) \, \text{dB} \qquad (1)$$

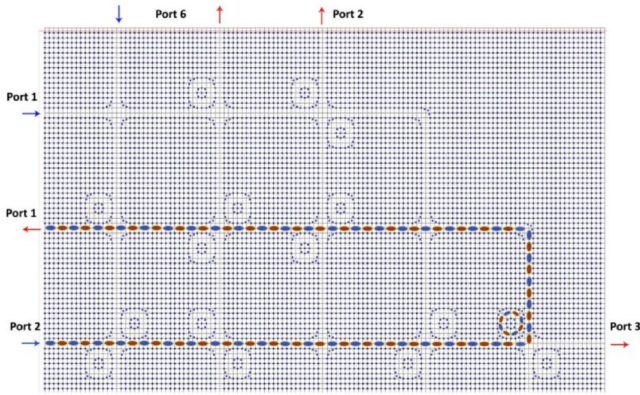$$\text{Insertion loss (dB)} = -(T_x) \, \text{dB} \qquad (2)$$

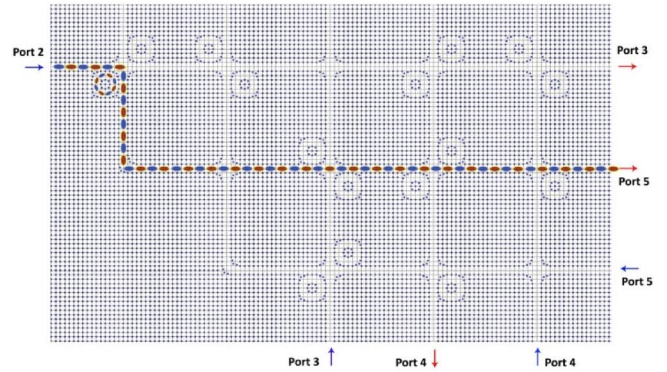**FIGURE 4** Propagation of signal $\lambda_5 = 1.52$ μm from port 2 to port 1 using ring resonator 'E'

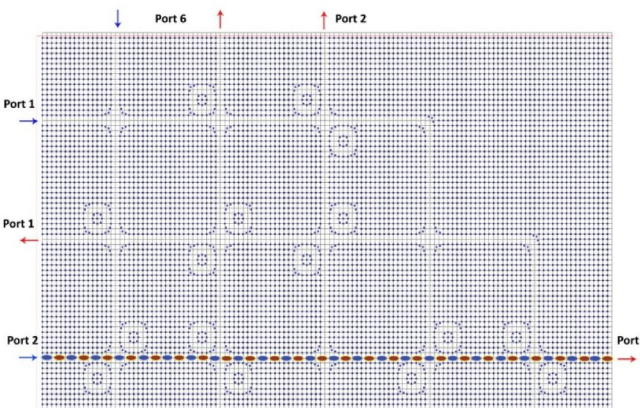**FIGURE 7** Propagation of signal $\lambda_1 = 1.49$ μm from port two to port five using ring resonator 'G'

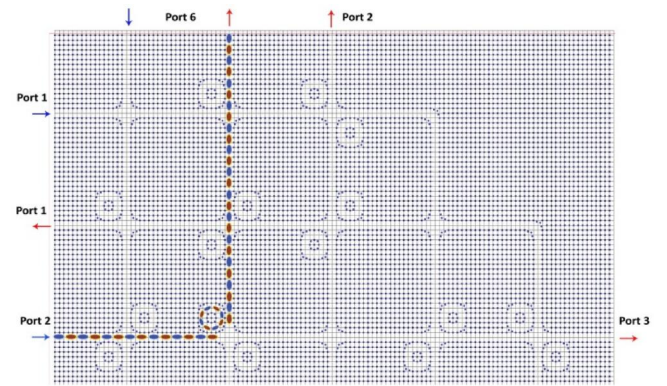**FIGURE 5** Propagation of signal $\lambda_3 = 1.48$ μm from port 2 to port 3 without any ring resonator

FIGURE 8 Propagation of signal $\lambda_4 = 1.51$ μm from port 2 to port 6 using ring resonator 'H'

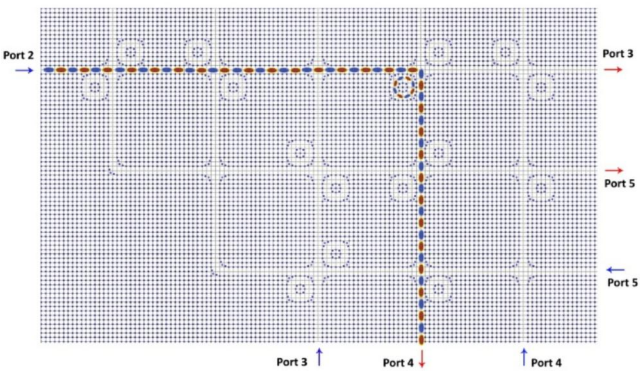**FIGURE 6** Propagation of signal $\lambda_2 = 1.5$ μm from port 2 to port 4 using ring resonator 'F'

where, T_i, T_t and T_x are the transmittance of isolated ports, through ports and port X.

Figure 9 shows the spectrum of desired signals obtained from all the output ports when each port acts as an input. Figure 10 shows the transmittance and crosstalk at output ports when input is excited at the port 2 of the router. For

this proposed 6 × 6 router, a total of 36 outputs is obtained considering each port as an input port. Table 3 gives the values of insertion loss and propagation delay of the 6 × 6 wavelength router. The propagation delay for the router is in terms of nanoseconds and the highest delay of 0.81 ns is achieved for the pathway between ports 2 and port 1. In terms of crosstalk (CT), considering port 1 as input port the maximum values of CT obtained are $CT_{45} = -13.5044$ dB, which is the CT between the through port 4 and isolated port 5. The minimum values obtained is for $CT_{23} = -24.6283$ dB. With port 2 as input port the maximum and minimum values of CT occurs between $CT_{16} = -14.7373$ dB, $CT_{41} = -29.0553$ dB and $CT_{51} = -29.8722$ dB. CT_{41} and CT_{51} have approximately the same values of crosstalk. For port 3 as input, $CT_{42} = -12.3553$ dB obtains maximum CT, whereas CT_{62} and CT_{64} share the minimum CT values as -22.8105 dB. The highest and lowest range of CT obtained for port 4 as input port are $CT_{56} = -25.8252$ dB and $CT_{26} = -13.2951$ dB. Port 5 as input port have a maximum value of $CT_{13} = -15.7054$ dB and minimum values as $CT_{12} = -29.6848$ dB and $CT_{42} = -29.9519$ dB. Finally, port
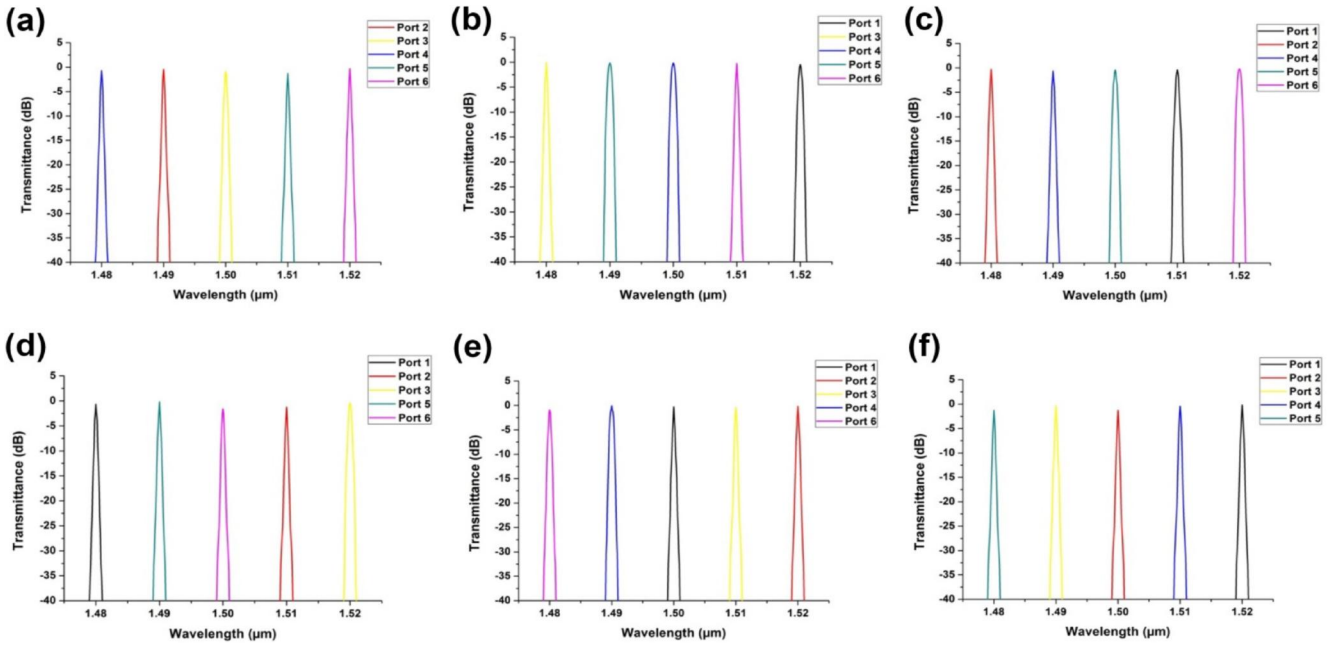
FIGURE 9 Transmittance of signals from output ports: (a) port 1 as input, (b) port 2 as input, (c) port 3 as input, (d) port 4 as input, (e) port 5 as input, and (f) port 6 as input
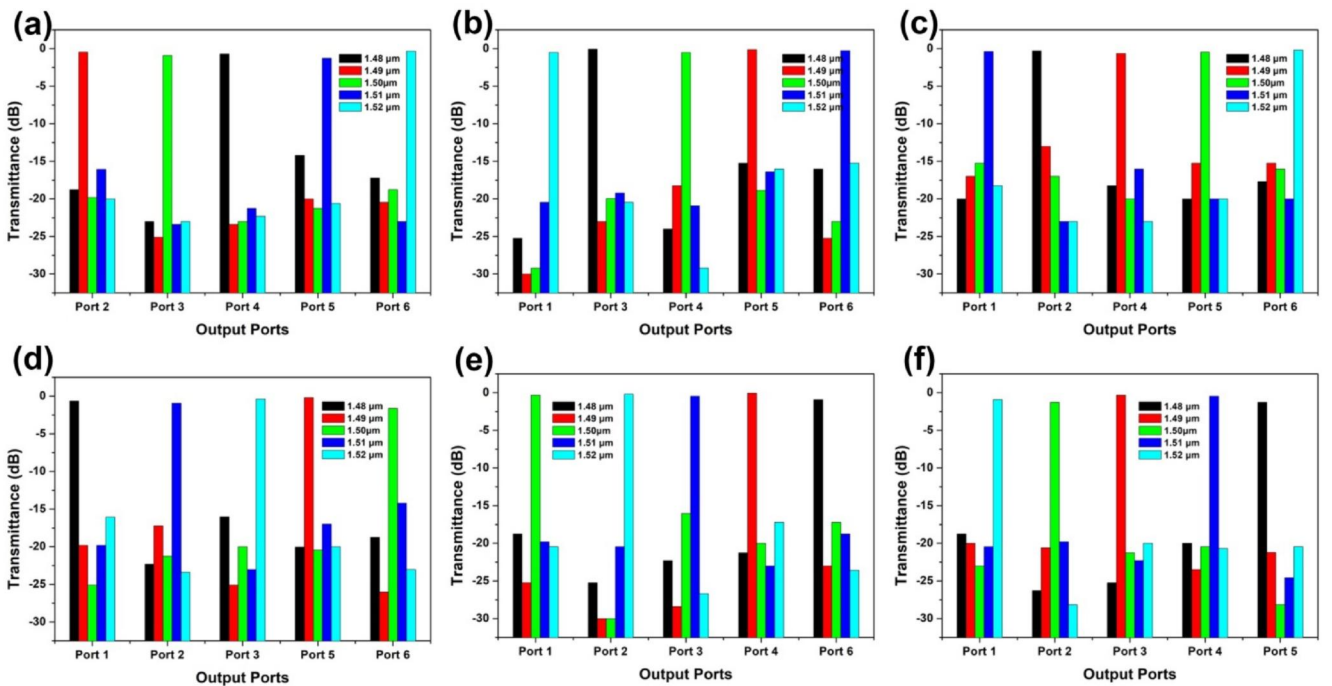
FIGURE 10 Transmittance and crosstalk of signals at output ports: (a) port 1 as input, (b) port 2 as input, (c) port 3 as input, (d) port 4 as input, (e) port 5 as input, and (f) port 6 as input

6 as an input port, the maximum and minimum values of CT obtained during the simulation is $CT_{51} = -17.498$ dB and $CT_{12} = -27.9577$ dB. All the values are tabulated in Table 4. The parameters of the devised structure along with the existing photonic crystal routers are shown in Table 5.

From Table 5, it is noted that different group of researchers has reported PCRR-based routers operating around the third optical window wavelength. We have designed a higher order 6 × 6 wavelength router due to the increase in demand for routing between large number of input and output

TABLE 3 Parameter metrics of 6 × 6 wavelength router

Input port	Output port	Routing wavelength (µm)	IL (dB)	Propagation delay (ns)
1	2	1.49	0.4581	0.2131
	3	1.50	0.9151	0.2337
	4	1.48	0.7058	0.2510
	5	1.51	1.2569	0.6709
	6	1.52	0.3152	0.1732
2	1	1.52	0.4915	0.8100
	3	1.48	0.0833	0.1320
	4	1.50	0.1529	0.6411
	5	1.49	0.1278	0.7513
	6	1.51	0.2733	0.6321
3	1	1.51	0.3858	0.2710
	2	1.48	0.2919	0.1210
	4	1.49	0.6550	0.6132
	5	1.50	0.4576	0.2109
	6	1.52	0.2000	0.5719
4	1	1.48	0.6550	0.4150
	2	1.51	0.9151	0.4310
	3	1.52	0.3858	0.4010
	5	1.49	0.1954	0.3971
	6	1.50	1.6115	0.5678
5	1	1.50	0.3152	0.6103
	2	1.52	0.1954	0.3510
	3	1.51	0.4581	0.7310
	4	1.49	0.0480	0.2828
	6	1.48	0.9151	0.1970
6	1	1.52	0.1954	0.2912
	2	1.50	1.2569	0.4997
	3	1.49	0.3152	0.5320
	4	1.51	0.4581	0.4810
	5	1.48	1.2569	0.2013

TABLE 4 Crosstalk values in 6 × 6 wavelength router

Input port	Maximum crosstalk (dB)	Minimum crosstalk (dB)
1	$CT_{45} = -13.5044$	$CT_{23} = -24.6283$
2	$CT_{16} = -14.7373$	$CT_{41} = -29.0553$
		$CT_{51} = -29.8722$
3	$CT_{42} = -12.3553$	$CT_{62} = -22.8105$
		$CT_{64} = -22.8105$
4	$CT_{26} = -13.2951$	$CT_{56} = -25.8252$
5	$CT_{13} = -15.7054$	$CT_{12} = -29.6848$
		$CT_{42} = -29.9519$
6	$CT_{51} = -17.4980$	$CT_{12} = -27.9577$

ports and an increasing number of users. The parameters such as operating wavelength, crosstalk, insertion loss, delay, and area of the devised structure have been given in the table.

5 | CONCLUSION

In summary, photonic crystal based 6 × 6 router has been demonstrated for the first time to the best of our knowledge. The photonic router is designed based on PCRRs. The evaluation result of the designed structure based on FDTD shows that the 6 × 6 router achieves acceptable performance measures in terms of crosstalk, insertion loss, and propagation delay. The highest crosstalk, insertion loss, and

TABLE 5 Comparison of proposed photonic crystal ring resonator with the existing reported router structures

Authors	$N \times N$	Resonated λ (μm)	Maximum insertion loss (dB)	Maximum crosstalk (dB)	Propagation delay (ps)	Area (μm^2)
Calo et al. [17]	4×4	1.488	0.6	−15.4	0.2	900
		1.506	0.1	−13.9	0.2	
		1.540	0.3	−15.7	0.1	
Calo et al. [18]	4×4	1.5000	0.160	−20.77	–	576
		1.5070	0.167	−22.37	–	
		1.5137	0.409	−20.13	–	
	4×4	1.540	0.36	−14.24	–	
		1.546	1.40	−10	–	
		1.550	0.47	−17.52	–	
Sridarshini et al. [3]	1×2	1.50	0.8882	−9.1118	0.00037	82.15
		1.52	0.2229	−19.9999	0.00035	
	3×3 (topology 1)	1.50	0.9151	−16.2973	0.0021	524.88
		1.52	0.7058	−20.4096	0.0005	
		1.54	1.8709	−16.8883	0.00214	
	3×3 (topology 2)	1.50	2.5026	−13.5485	0.00101	428.49
		1.52	1.9540	−19.3254	0.00086	
Sathyadevaki et al. [19]	1×2 and 2×2 router	1518	1.950152	−30.2488	3.7	182
		1550	2.76605	−19.845	0.8	
		1530	5.944498	−26.5422	0.5	
	$R = 0.2778*$ a (1×2 and 2×2 router)	1520	0.72724	−30.6485	0.6	182
		1559	2.62596	−17.5205	2.4	
		1542	4.11024	−15.0619	2.0	
	4×4 router	1518	0.98436	−20.8124	0.5	1216
		1550	0.35402	−22.1843	4.6	
	Increased radii 4×4 router	1529	2.41	−33.4683	4.6	1216
		1520	1.734322	−21.3637	2.02	
		1559	5.10545	−23.5218	0.6	
Proposed router	**6×6**	**1.48**	**1.2569**	**−13.5044**	**415.0**	**4900**
		1.49	**0.6550**	**−12.3553**	**751.3**	
		1.5	**1.6115**	**−14.7712**	**641.1**	
		1.51	**1.2569**	**−13.2951**	**731.0**	
		1.52	**0.4915**	**−15.6644**	**810.0**	

Note: The paramater values of the designed 6×6 router structure in table 5 has been mentioned in bold as to highlight it from the already reported structures.

propagation delay obtained in this reported structure are −12.3553 dB, 1.6115 dB, and 810 ps. In spite of the complex 6×6 router structure, the main advantage of the reported design is that the routing path for any input-output port configuration will encounter only one ring resonator or no resonator at all. And also the routing path between the input and output ports depends on the location of the ring resonators along the path. Thus, the routing path can be designed based on the requirement of the application. Moreover, the ultra-compact size of the router 4900 μm^2 will make it a candidate applicable for a fully integrated optical circuit in the future of telecommunication industries.

ORCID

Sridarshini Thirumaran https://orcid.org/0000-0001-9922-4378

Shanmuga Sundar Dhanabalan https://orcid.org/0000-0001-5539-3380

REFERENCES

1. Liu, L., et al.: On-chip passive three-port circuit of all-optical ordered-route transmission. Sci. Rep. 5, 1–9 (2015)
2. Sridarshini, T., Gandhi, S.I.: Compact 3 × 3 wavelength routing for photonic integrated circuits. Photonic Netw. Commun. 36(1), 68–81 (2018)
3. Sridarshini, T., Gandhi, I., Rakshitha, M.: Design and analysis of 1xN symmetrical optical splitters for photonic integrated circuits. Optik. 169, 321–331 (2018)
4. Djavid, M., et al.: Photonic crystal power dividers using L-shaped bend based on ring resonators. J. Opt. Soc. Am. B. 25(8), 1231–1235 (2008)
5. Sundar, D.S., et al.: Compact four-port circulator based on 2D photonic crystals with a 90° rotation of the light wave for photonic integrated circuits applications. Laser Phys. 29(6), 066201 (2019)
6. Sathyadevaki, R., Shanmuga sundar, D, Sivanantha Raja, A.: Design of dual ring wavelength filters for WDM applications. Opt. Commun. 380, 409–418 (2016)
7. Daghooghi, T., Soroosh, M., Ansari-Asl, K.: Ultra-fast all-optical decoder based on nonlinear photonic crystal ring resonators. Appl. Opt. 57(9), 2250–2257 (2018)
8. Hadadan, F., Soroosh, M.: A new proposal for 4-to-2 optical encoder using nonlinear photonic crystal ring resonators. Int. J. Opt. Photonics. 13, 119–126 (2019)
9. Haddadan, F., Soroosh, M.: Low-power all-optical 8-to-3 encoder using photonic crystal-based waveguides. Photonic Netw. Commun. 37(1), 83–89 (2019)
10. Haddadan, F., Soroosh, M., Alaei-Sheini, N.: Designing an electro-optical encoder based on photonic crystals using the graphene–Al 2 O 3 stacks. Appl. Opt. 59(7), 2179–2185 (2020)
11. Sherwood-Droz, N., et al.: Optical 4x4 hitless Silicon router for optical Networks-on-Chip (NoC): erratum. Opt. Express. 16(23), 19395 (2008)
12. Lu, J., et al.: Wavelength routers with low crosstalk using photonic crystal point defect micro-cavities. Optik. 127(6), 3235–3242 (2016)
13. Zhihua, Y., et al.: Microring resonator-based optical router for photonic networks-on-chip. Quantum Electron. 46(7), 655 (2016)
14. Kaźmierczak, A., et al.: Highly integrated optical 4 × 4 crossbar in silicon-on-insulator technology. J. Light. Technol. 27(16), 3317–3323 (2009)
15. Kirman, N., Martínez, J.F.: A power-efficient all-optical on-chip interconnect using wavelength-based oblivious routing. In: International Conference on Architectural Support for Programming Languages and Operating Systems-ASPLOS (2010)
16. Ji, R., et al.: Five-port optical router for photonic networks-on-chip. Opt. Express. 19(21), 20258–20268 (2011)
17. Calo, G., Petruzzelli, V.: Wavelength routers for optical networks-on-chip using optimized photonic crystal ring resonators. IEEE Photonics J. 5(3), 7901011 (2013)
18. Calò, G., Petruzzelli, V.: Compact design of photonic crystal ring resonator 2×2 routers as building blocks for photonic networks on chip. J. Opt. Soc. Am. B. 31(3), 517–525 (2014)
19. Sathyadevaki, R., Sundar, D.S., Raja, A.S.: Photonic crystal 4 × 4 dynamic hitless routers for integrated photonic NoCs. Photonic Netw. Commun. 36(1), 82–95 (2018)
20. Shanmuga Sundar, D., et al.: Photonic crystal based routers for photonic integrated on chip networks: a brief analysis. Opt. Quantum Electron. 50(11), 1–15 (2018)
21. Lu, T.W., et al.: Square lattice photonic crystal point-shifted D0 nanocavity with lowest-order whispering-gallery mode. In: Optics InfoBase Conference Papers (2010)
22. Joannopoulos, J.D., et al.: Photonic crystals: Molding the flow of light. Princeton University Press, Princeton, NJ (2011)
23. Chih Jung, W., Ping Liu, C., Zhengbiao, O.: Compact and low-power optical logic NOT gate based on photonic crystal waveguides without optical amplifiers and nonlinear materials. Appl. Opt. 51(5), 680–685 (2012)